

# 2HDM Neutral Scalars under the LHC

Felix Kling\*

SLAC National Accelerator Laboratory, 2575 Sand Hill Road, Menlo Park, CA 94025, USA

Shufang Su†

Department of Physics, University of Arizona, Tucson, AZ 85721, USA

Wei Su‡

ARC Centre of Excellence for Particle Physics at the Terascale,  
Department of Physics, University of Adelaide, South Australia 5005, Australia

Two Higgs Doublet Models (2HDM) provide a simple framework for new physics models with an extended Higgs sector. The current LHC results, including both direct searches for additional non-Standard Model (SM) Higgs bosons, as well as precision measurements of the SM-like Higgs couplings, already provide strong constraints on the 2HDM parameter spaces. In this paper, we examine those constraints for the neutral scalars in the Type-I and Type-II 2HDM. In addition to the direct search channels with SM final states:  $H/A \rightarrow f\bar{f}, VV, Vh, hh$ , we study in particular the exotic decay channels of  $H/A \rightarrow AZ/HZ$  once there is a mass hierarchy between the non-SM Higgses. We found that  $H/A \rightarrow AZ/HZ$  channel has unique sensitivity to the alignment limit region which remains unconstrained by conventional searches and Higgs precision measurements. This mode also extends the reach at intermediate  $t_\beta$  for heavy  $m_A$  that are not covered by the other direct searches.

## CONTENTS

I. Introduction	1
II. The 2HDM	2
III. Collider Constraints on BSM Higgses	3
IV. Degenerate Higgs Masses	4
V. Non-degenerate Case: $H/A \rightarrow AZ/HZ$	5
A. $m_A$ vs. $m_H$	6
B. $\tan\beta$ vs. $\cos(\beta - \alpha)$	6
C. $\tan\beta$ vs. $m_A$	9
VI. Conclusion and Outlook	9
Acknowledgments	11
References	11

## I. INTRODUCTION

Since the discovery of the Standard Model (SM)-like 125 GeV Higgs boson at the first run of the Large Hadron Collider (LHC) [1, 2], the SM is confirmed to be a self-consistent theory. Meanwhile motivated by various experimental observations and theoretical considerations, such as the existence of dark matter, the baryon asymmetry of the universe, the strong CP problem, the muon

$g-2$  anomaly, or the naturalness problem, searches for new physics beyond the SM still remain a frontier in particle physics research.

Many of the proposed new physics models contain an extended Higgs sector, among which the Two Higgs Doublet Model (2HDM) is one of the simplest options. After electroweak symmetry breaking (EWSB), the general CP-conserving 2HDM contains five physical eigenstates: the observed 125 GeV CP-even neutral scalar  $h$ , an additional CP-even neutral scalar  $H$ , one CP-odd Higgs boson  $A$ , and a pair of charged Higgs boson  $H^\pm$  [3]. The discovery of any beyond the SM (BSM) Higgses will be an unambiguous evidence for the existence of an extended Higgs sector.

There are usually two ways to probe extended Higgs sectors: through their modifications to the SM-like Higgs couplings tested by Higgs coupling precision measurements [4], and direct searches for BSM Higgses at high energy colliders [5]. The current direct searches at the LHC include both conventional search channels of  $H/H^\pm/A \rightarrow f\bar{f}, VV'$ , as well as final states involving a SM-like Higgs  $H \rightarrow Vh, hh$ . Under the alignment limit of the 2HDM, in which the 125 GeV Higgs  $h$  is exactly SM-like, both the decays  $H \rightarrow VV$  and  $H \rightarrow Vh, hh$  as well as the  $VH$  and WBF production modes vanish at tree level, making a discovery more challenging. However, if there is a mass hierarchy between the BSM Higgses, additional exotic decay modes, such as  $H/A \rightarrow AZ/HZ, H/A \rightarrow H^\pm W^\mp, H \rightarrow AA, H^+ H^-$  or  $H^\pm \rightarrow HW/AW$  open up and quickly dominate the decay branching fractions. Such exotic decay modes open a new window to search for heavy BSM Higgses. Meanwhile current collider limits on heavy Higgses would be relaxed given the suppression of their decay branching fractions. In this paper we comprehensively examine

\* felixk@slac.stanford.edu

† shufang@email.arizona.edu

‡ wei.su@adelaide.edu.au

the current constraints on the 2HDM parameter space in mass-degenerate and hierarchical scenarios, highlighting the complementarity and importance of the exotic Higgs decay channel  $H/A \rightarrow HZ/AZ$ .

The rest of the paper is organized as follows. We will give a brief introduction to 2HDM at Sec. II and compare the Type-I and Type-II. In Sec. III, we summarize the latest LHC searches that are relevant for Higgs studies. We show our interpreted results for the Type-I and Type-II 2HDM under the degenerate mass assumption in Sec. IV. In Sec. V we extend this discussion to 2HDMs with non-degenerate mass spectra, focusing on the exotic decay channel of  $H/A \rightarrow AZ/HZ$ . We conclude in Sec. VI.

## II. THE 2HDM

The scalar sector of the 2HDM consists of two  $SU(2)$  doublets  $\Phi_i$ ,  $i = 1, 2$ , which can be parameterized as

$$\Phi_i = \begin{pmatrix} \phi_i^+ \\ (v_i + \phi_i^0 + i\varphi_i)/\sqrt{2} \end{pmatrix}. \quad (1)$$

Here  $v_i$  are the vacuum expectation values for the neutral components which satisfy the condition  $v_1^2 + v_2^2 = v^2$  with  $v = 246$  GeV. After imposing a discrete  $\mathcal{Z}_2$  symmetry on the Lagrangian to avoid tree-level flavour changing neutral currents (FCNCs), the 2HDM parameter space is described by six free parameters. For our purposes it is convenient to parameterize the 2HDM by the physical Higgs masses ( $m_h, m_H, m_A$  and  $m_{H^\pm}$ ), the mixing angle between the two CP-even Higgses ( $\alpha$ ), and the ratio of the two vacuum expectation values ( $t_\beta = v_2/v_1$ ). If we allow for a soft breaking of the  $\mathcal{Z}_2$  symmetry, there is an additional parameter  $m_{12}^2$ .

After EWSB, the scalar sector consists of five states: a pair of neutral CP-even Higgses,  $h$  and  $H$ , a CP-odd Higgs,  $A$ , and a pair of charged Higgses  $H^\pm$ . For the neutral states we can write

$$\begin{aligned} h &= -s_\alpha \phi_1^0 + c_\alpha \phi_2^0, \\ H &= c_\alpha \phi_1^0 + s_\alpha \phi_2^0, \\ A &= -s_\beta \varphi_1 + c_\beta \varphi_2, \end{aligned} \quad (2)$$

where we used the shorthand notation  $s_x = \sin x$  and  $c_x = \cos x$ . In the following we will identify  $h$  with the discovered 125 GeV Higgs<sup>1</sup>. Note that in the generic 2HDM, Higgs masses are free parameters and therefore exotic Higgs decays such as  $A \rightarrow HZ$  are possible when kinetically accessible.

In the context of this paper, we are mainly interested in the couplings of the neutral Higgses to the SM gauge bosons  $V = Z, W^\pm$ . The couplings of the neutral CP-even Higgses to a pair of vector bosons are

$$g_{hVV} = \frac{m_V^2}{v} s_{\beta-\alpha} \quad \text{and} \quad g_{HVV} = \frac{m_V^2}{v} c_{\beta-\alpha}, \quad (3)$$

while the CP-odd Higgs  $A$  does not couple to vector boson pairs. Additionally, the neutral CP-even Higgses can couple to the CP-odd Higgs  $A$  and a  $Z$ -boson with couplings

$$\begin{aligned} g_{hAZ} &= \frac{g c_{\beta-\alpha}}{2c_{\theta_W}} (p_h - p_A)_\mu \quad \text{and} \\ g_{HAZ} &= -\frac{g s_{\beta-\alpha}}{2c_{\theta_W}} (p_H - p_A)_\mu, \end{aligned} \quad (4)$$

where  $\theta_W$  is the Weinberg angle and  $p_\mu$  are the incoming Higgs momenta. LHC Higgs coupling measurements favor the *alignment limit*,  $s_{\beta-\alpha} \approx 1$ , in which the couplings of the 125 GeV Higgs to fermions and gauge bosons are consistent with those predicted by the SM [3, 6–9]. In this case, the coupling of the BSM CP-even neutral Higgs  $H$  to vector boson pairs is suppressed by  $c_{\beta-\alpha} \approx 0$ , which is consistent with the non-observation of such a state in the  $H \rightarrow VV$  channel [10, 11]. On the other hand, in the alignment limit, the CP-odd Higgs will couple more strongly to the BSM Higgs  $H$  than its SM-like counterpart  $h$ . In particular, this implies that  $A$  is more likely to decay to  $HZ$  than  $hZ$ , if kinematically possible. This motivates the exotic Higgs searches for  $A \rightarrow HZ$  and  $H \rightarrow AZ$  as complementary probe in the alignment limit.

Unlike the couplings to fermions and vector bosons, the triple and quartic Higgs couplings depend on the otherwise unobservable soft  $\mathcal{Z}_2$  breaking parameter  $m_{12}^2$ . The corresponding expressions for various triple Higgs couplings have been obtained in [12]. However, it has been shown in Ref. [13] that satisfying unitarity and vacuum stability bounds for arbitrary values of  $t_\beta$  requires  $m_{12}^2 = m_H^2 s_\beta c_\beta$ , with deviations possible only at  $t_\beta \sim 1$ . For illustration, we consider that this relation holds, in which case we can write the triple Higgs couplings as

$$\begin{aligned} g_{Hhh} &= -\frac{c_{\beta-\alpha}}{v} \frac{s_{2\alpha}}{s_{2\beta}} (m_H^2 - m_h^2) + \frac{c_{\beta-\alpha}}{2v} m_H^2, \\ g_{HAA} &= -\frac{c_{\beta-\alpha}}{2v} (m_H^2 - 2m_A^2), \\ g_{hhh} &= -\frac{c_{\beta-\alpha}^2}{v} \left[ \frac{c_{\beta-\alpha}}{t_{2\beta}} - s_{\beta-\alpha} \right] (m_H^2 - m_h^2) + \frac{s_{\beta-\alpha}}{2v} m_h^2, \\ g_{hAA} &= -\frac{s_{\beta-\alpha}}{2v} [2(m_H^2 - m_A^2) - m_h^2] - \frac{c_{\beta-\alpha}}{t_{2\beta} v} (m_H^2 - m_h^2). \end{aligned} \quad (5)$$

We can see that in the alignment limit  $c_{\beta-\alpha} = 0$ , the decays of the heavy neutral Higgs  $H \rightarrow hh, AA$  are absent and the SM Higgs self coupling obtains its SM value  $g_{hhh} = m_h^2/(2v)$ , while a decay of  $h \rightarrow AA$  is possible if kinematically open.

As mentioned above, we have introduced a soft breaking  $\mathcal{Z}_2$  symmetry to avoid tree-level FCNCs, which implies that each fermion type is only allowed to couple

<sup>1</sup> Note that here we use a convention in which  $h$  is always the 125 GeV SM-like Higgs and the alignment limit is always at  $c_{\beta-\alpha} = 0$ . This is different from the mass ordered convention in which  $h$  is the light CP-even Higgs and  $H$  is the heavy one.

2HDM	Type-I	Type-II	Type-L	Type-F
up-type	$\Phi_2$	$\Phi_2$	$\Phi_2$	$\Phi_2$
$\xi_{h uu}$	$c_\alpha/s_\beta$	$c_\alpha/s_\beta$	$c_\alpha/s_\beta$	$c_\alpha/s_\beta$
$\xi_{H uu}$	$s_\alpha/s_\beta$	$s_\alpha/s_\beta$	$s_\alpha/s_\beta$	$s_\alpha/s_\beta$
$\xi_{A uu}$	$t_\beta^{-1}$	$t_\beta^{-1}$	$t_\beta^{-1}$	$t_\beta^{-1}$
down-type	$\Phi_2$	$\Phi_1$	$\Phi_2$	$\Phi_1$
$\xi_{h dd}$	$c_\alpha/s_\beta$	$-s_\alpha/c_\beta$	$c_\alpha/s_\beta$	$-s_\alpha/c_\beta$
$\xi_{H dd}$	$s_\alpha/s_\beta$	$c_\alpha/c_\beta$	$s_\alpha/s_\beta$	$c_\alpha/c_\beta$
$\xi_{A dd}$	$-t_\beta^{-1}$	$t_\beta$	$-t_\beta^{-1}$	$t_\beta$
lepton	$\Phi_2$	$\Phi_1$	$\Phi_1$	$\Phi_2$
$\xi_{h \ell \ell}$	$c_\alpha/s_\beta$	$-s_\alpha/c_\beta$	$-s_\alpha/c_\beta$	$c_\alpha/s_\beta$
$\xi_{H \ell \ell}$	$s_\alpha/s_\beta$	$c_\alpha/c_\beta$	$c_\alpha/c_\beta$	$s_\alpha/s_\beta$
$\xi_{A \ell \ell}$	$-t_\beta^{-1}$	$t_\beta$	$t_\beta$	$-t_\beta^{-1}$

TABLE I. Types of 2HDM and the tree-level couplings of  $h$ ,  $H$  and  $A$  to fermions, normalized to their SM Yukawa couplings:  $\xi = y/y^{SM}$ .

to one Higgs doublet. There are four possible types of 2HDMs: Type-I, Type-II, Type-L (or lepton-specific) and Type-F (or flipped), which we show in Tab. I. The corresponding couplings of the neutral scalar states to SM fermions normalized to their SM values, can be expressed in terms of the mixing angles  $\alpha$  and  $\beta$  and are also shown in Tab. I. For the remainder of this paper we focus on 2HDMs of Type-I and Type-II, and the main differences of the interpreted results come from the BSM Higgs couplings to fermion pairs.

### III. COLLIDER CONSTRAINTS ON BSM HIGGSSES

A variety of LHC measurements can be used to constrain extended Higgs sectors such as 2HDMs. This includes indirect constraints from precision Higgs couplings, direct searches for additional Higgses as well as measurements of SM processes. In the following we summarize the different searches and measurements that we use for our analyses. Here we mostly focus on the neutral scalars, and comment on the charged scalar at the end.

**Precision Higgs Measurements:** While the couplings of the 125 GeV Higgs  $h$  are fixed in the SM, they are modified in the 2HDM: at tree level they depend on the mixing angles  $c_{\beta-\alpha}$  and  $t_\beta$ , while additional dependence on the Higgs masses is induced via loop effects [6–10, 14]. We use the latest combined LHC 13 TeV measurements of the Higgs coupling strength at both CMS with  $36 \text{ fb}^{-1}$  [15] and ATLAS with  $80 \text{ fb}^{-1}$  [4].

Additionally, the Higgs width has been measured with high precision:  $0.08 \text{ MeV} < \Gamma_h < 9.16 \text{ MeV}$  at 95% C.L., by CMS [16]. This measurement put strong constraints on both the enhanced couplings of  $h$  to fermions at high/low  $t_\beta$  and additional decay modes such as  $h \rightarrow AA$ .

**Conventional channels:** Most of the existing direct searches for BSM Higgs bosons focus on their conventional decays into a pair of quarks, leptons or gauge bosons. The following table presents a summary of recent searches performed at the 13 TeV LHC.

channel	CMS	ATLAS
$A/H \rightarrow \mu\mu$	[17]	[18]
$A/H \rightarrow bb$	[19]	[20]
$A/H \rightarrow \tau\tau$	[21, 22]	[23]
$A/H \rightarrow \gamma\gamma$	[24, 25]	[26–28]
$A/H \rightarrow tt$	[29]	-
$H \rightarrow ZZ$	[30]	[31]
$H \rightarrow WW$	[32]	[33]

Note that the  $gg \rightarrow A/H \rightarrow tt$  channel involves a non-trivial interference with the SM backgrounds that has been taken into account in the analysis. A brief summary of Higgs search results can be found in Ref. [34] for CMS at 8 TeV and Ref. [35] for ATLAS at 13 TeV.

**Exotic Decays into the SM Higgs:** Away from the alignment limit  $c_{\beta-\alpha} = 0$ , the heavy CP-odd Higgs can decay into the SM-like Higgs via  $A \rightarrow hZ$ . Additionally, the heavy CP-even Higgs can decay into a pair of SM-like Higgses,  $H \rightarrow hh$ . In our analysis we take into account the search results listed in the following table, where for the resonant di-Higgs channel, we consider the limits resulting from the combination of different final states.

channel	ATLAS		CMS	
	8 TeV	13 TeV	8 TeV	13 TeV
$A \rightarrow hZ \rightarrow bb\ell\ell$	[36]	[37]	[38]	[39]
$A \rightarrow hZ \rightarrow \tau\tau\ell\ell$	[40]	[41]	[38]	—
$H \rightarrow hh$	[42]	[43]	[44]	[45]

**Exotic Decays of the SM Higgs:** If the BSM scalars are sufficiently light,  $m_{A/H} < m_h/2$ , exotic decays of the SM-like Higgs  $h \rightarrow AA/HH$  open up. While the decay  $h \rightarrow HH$  vanishes for  $c_{\beta-\alpha} = 0$ , the decay  $h \rightarrow AA$  is unsuppressed under the alignment limit. The following table lists the current LHC searches considered for such channels, focusing on masses of  $m_A > 4 \text{ GeV}$ . Searches listed in parenthesis do not provide the leading constraints and are only listed for completeness.

channel	ATLAS	CMS
$h \rightarrow AA \rightarrow bbbb$	[46]	—
$h \rightarrow AA \rightarrow bb\tau\tau$	—	[47]
$h \rightarrow AA \rightarrow bb\mu\mu$	[48]	[49]
$h \rightarrow AA \rightarrow \tau\tau\tau\tau$	—	[50]
$h \rightarrow AA \rightarrow \tau\tau\mu\mu$	[51]	[52]
$h \rightarrow AA \rightarrow \mu\mu\mu\mu$	([53])	([54])

A brief summary on search results for exotic decays of the SM-like Higgs can be found in Ref. [55] for CMS at 8 TeV and Ref. [56] for ATLAS at 13 TeV.

**Exotic Decays in BSM Sector:** If the two neutral BSM Higgs states  $A$  and  $H$  have a sufficient mass splitting,  $|m_A - m_H| > m_Z$ , the exotic decay channel  $A/H \rightarrow HZ/AZ$  opens up. Both ATLAS and CMS have performed searches listed in the following table.

channel	ATLAS	CMS
$A/H \rightarrow HZ/AZ \rightarrow b\bar{b}\ell\bar{\ell}$	[57] (13 TeV)	[58] (13 TeV)
$A/H \rightarrow HZ/AZ \rightarrow \tau\tau\ell\bar{\ell}$	—	[59] (8 TeV)

**LEP Searches:** The Large Electron-Positron Collider (LEP) performed searches for light BSM Higgs bosons both using the  $e^+e^- \rightarrow HZ$  and  $e^+e^- \rightarrow AH$  channel [60]. The  $HZ$  production rate scales proportionally to  $c_{\beta-\alpha}$  and the null results of this search can constrain  $c_{\beta-\alpha}$  down to about 0.1 for  $m_H$  between 12.5 to 114.4 GeV. This constraint does not apply to any of the benchmarks considered in this paper. In contrast, the double Higgs production channel  $AH$  is unsuppressed under the alignment limit and roughly constrains  $m_A + m_H \lesssim 200$  GeV.

**Measurements of SM processes:** In the absence of dedicated resonance searches, additional BSM Higgs states can also be probed through inclusive cross section measurements of rare SM processes. In this work, we consider two such processes: i) The exotic Higgs decay  $A/H \rightarrow HZ/AZ \rightarrow ttZ$ , which dominates for daughter Higgs masses above the di-top threshold, can be probed using the  $ttZ$  cross section measurement [61]. ii) The associated  $ttH/ttA$  production channel with subsequent decay  $H/A \rightarrow tt$  is sensitive to the  $4t$  production rate [62–64]. This search constrains low  $t_\beta < 1$  for  $m_{A/H} > 2m_t$ , where the Higgs width becomes very large,  $\Gamma/m > 0.2$  and hence no resonance search can be performed anymore.

While the above constraints focus on the neutral Higgs bosons, additional theoretical and experimental constraints arise for the charged Higgs bosons  $H^\pm$ .

**Precision Constraints:** Electroweak precision measurements [65, 66] require the charged Higgs mass to be close to the mass of one of the neutral Higgses,  $m_{H^\pm} \sim m_H$  or  $m_A$  or  $m_h$  [13].

**Direct Searches:** Searches for charged Higgses  $H^\pm$  have been performed through the decay channels  $H^\pm \rightarrow cs$  [67, 68],  $\tau\nu$  [69, 70] and  $tb$  [71, 72]. At large masses of  $m_{H^\pm} > m_t$ , constraints on these charged Higgs searches are typically weaker than their neutral counterparts, due to the suppressed  $tbH^\pm$  associated production cross section as well as large backgrounds. A notable exception are searches of light charged Higgs bosons via top decays  $t \rightarrow H^\pm b$ , which exclude the mass range  $m_{H^\pm} \lesssim m_t$  for the Type-II 2HDM and part of the parameter space for the Type-I 2HDM.

**Flavour Constraints:** Precision flavour observables, such as of the branching fraction of  $B$  mesons, provide indirect constraints on the charged scalars. Most

notably, the measured value for  $\text{BR}(b \rightarrow s\gamma)$  imposes a lower limit on the charged Higgs mass to be larger than  $\sim 600$  GeV in the Type-II 2HDM [66, 73]. However, we note that the interpretation of these flavour measurements are typically model dependent and contributions from additional BSM sectors could significantly modify and relax these constraints.

Given the above considerations, we do not consider any additional constraints related to the charged Higgs bosons and solely focus on the neutral Higgs sector in this paper.

#### IV. DEGENERATE HIGGS MASSES

To interpret the experimental results, we take the limits on cross section times branching fraction  $\sigma \times \text{BR}$  of the various channels mentioned above, as well as the measurements of Higgs couplings and  $\Gamma_h$  to directly constrain the 2HDM parameter space. We use the `SusHi` package [74] to calculate the production cross-section at NNLO level, and the `2HDMC` [75] code for Higgs decay branching fractions at tree level. In Fig. 1, we show the current collider limits in the 2HDM  $m_{H/A} - t_\beta$  plane, taking into account the constraints mentioned above. We assume degenerate heavy Higgs masses  $m_A = m_H = m_{H^\pm}$  such that exotic decays involving two BSM Higgses are not kinematically open. The mixing angle  $c_{\beta-\alpha}$  is fixed to be 0.1 for the Type-I 2HDM (left panel) and 0.05 for the Type-II 2HDM (right panel), based on the consideration of the SM-like Higgs coupling measurements. Non-zero values of  $c_{\beta-\alpha}$  are relevant for  $A \rightarrow Zh$ ,  $H \rightarrow hh$  and  $H \rightarrow VV$ . The soft  $\mathcal{Z}_2$  breaking parameter  $m_{12}^2$  is chosen to be  $m_{12}^2 = m_H^2 s_\beta c_\beta$  to satisfy theoretical consideration of unitarity and vacuum stability.

For the Type-I 2HDM (left panel), current direct searches are mostly sensitive at  $t_\beta < 10$ . This is because the main production modes, gluon fusion and  $b$ -associated production, are both  $\cot\beta$ -enhanced from bottom and top Yukawa couplings. The limits from the conventional modes of  $A/H \rightarrow \tau\tau$  (orange) and  $A/H \rightarrow \gamma\gamma$  (brown) have weak dependence on the value of  $c_{\beta-\alpha}$  and exclude the low mass region below the top threshold of  $m_{A/H} \lesssim 2m_t$  for  $t_\beta < 3$ . Once the  $tt$  mode (magenta) is open, it quickly dominates the decay branching fractions. The region of  $400 \text{ GeV} < m_{A/H} < 750 \text{ GeV}$  with  $0.2 < t_\beta < 1$  is currently excluded by this channel. For even smaller  $t_\beta$ , no limits are quoted for the  $tt$  channel because the corresponding Higgs width is so wide that the resonant search results are not applicable [29, 76].

The limits for  $H \rightarrow VV$  (red),  $A \rightarrow Zh$  (blue), and  $H \rightarrow hh$  (green) strongly depend on the value of  $c_{\beta-\alpha}$  and vanish under the alignment limit of  $c_{\beta-\alpha} = 0$ . For  $c_{\beta-\alpha} = 0.1$ ,  $m_{A/H}$  between 200 and 850 GeV for  $0.5 < t_\beta < 10$  are excluded, with a gap at intermediate masses around 450 GeV for  $A \rightarrow Zh$  and  $H \rightarrow VV$  channel.

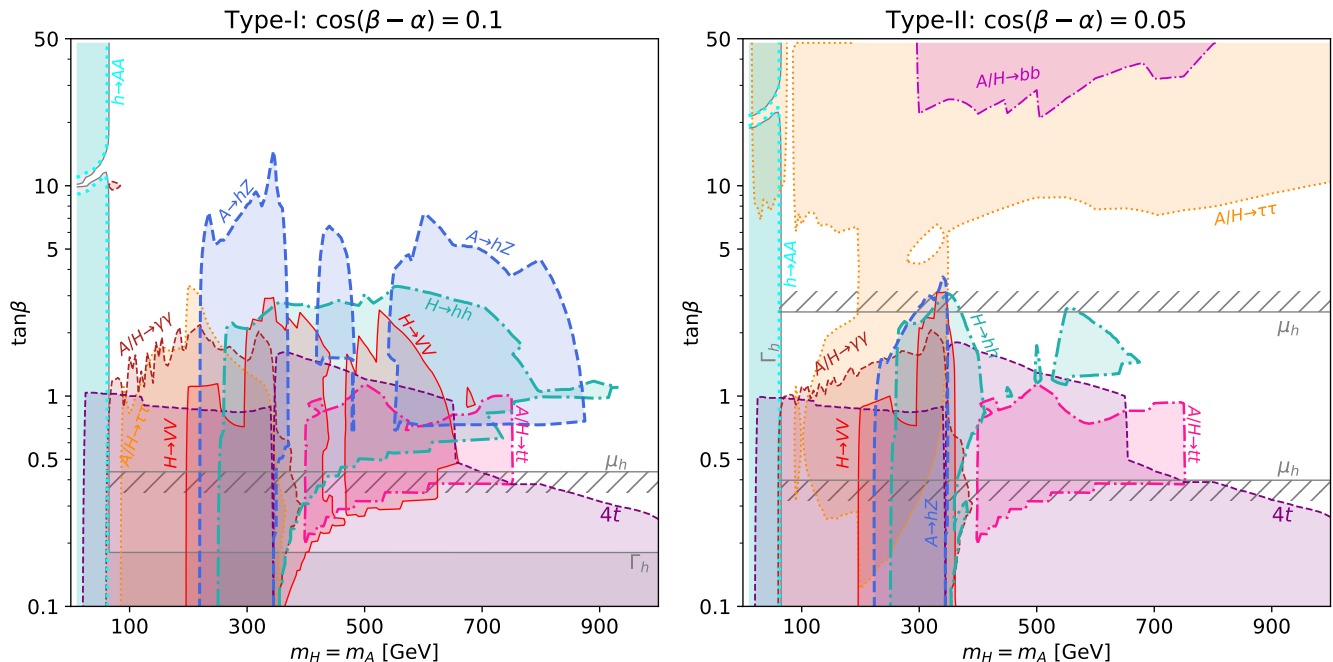


FIG. 1. Constraints for degenerate heavy Higgs mass spectrum  $m_A = m_H = m_{H^+}$ . We show the 95% C.L. exclusion region in the  $m_{A/H}$  vs.  $t_\beta$  plane on the Type-I 2HDM with  $c_{\beta-\alpha} = 0.1$  (left) and Type-II 2HDM with  $c_{\beta-\alpha} = 0.05$  (right) originating from i) the measurement of the Higgs width  $\Gamma_h$  (grey), ii) the conventional search results on  $H/A \rightarrow \tau\tau$  (dotted orange),  $H/A \rightarrow bb$  (dot-dashed pink),  $H \rightarrow VV$  (red),  $H/A \rightarrow \gamma\gamma$  (dashed brown),  $H/A \rightarrow tt$  (dot-dashed magenta) and  $4t$  production (dashed purple), and iii) exotic decay channels  $A \rightarrow hZ$  (dashed dark blue),  $H \rightarrow hh$  (dot-dashed green) and  $h \rightarrow AA$  (dotted cyan). Region enclosed by the grey hatched line are excluded at 95% CL. by the current Higgs coupling measurements.

The 95% C.L. range of the SM-like Higgs decay width (grey) excludes the low mass region of  $A/H$  given the opening of  $h \rightarrow AA$ ,  $HH$  for  $m_{A/H} < m_h/2$ , as well as low  $t_\beta$  region of  $t_\beta \lesssim 0.2$  for  $c_{\beta-\alpha} = 0.1$  due to the enhancement of fermion Yukawa couplings. A thin slice of surviving region from  $\Gamma_h$  constraints around  $t_\beta \sim 10$  remains due to the vanishing of  $\Gamma(h \rightarrow AA)$  in that region. Additionally, a global fit to the LHC SM-like Higgs coupling measurements excludes  $t_\beta \lesssim 0.4$  for  $c_{\beta-\alpha} = 0.1$ . Finally, the measurement of the four top production (purple) rate is sensitive to  $ttH/ttA$  associated production with  $A/H \rightarrow tt$ , constraining a wide region at low  $t_\beta$ .

For the Type-II 2HDM (right panel), the results are quite different at large  $t_\beta$  due to the  $t_\beta$ -enhanced bottom and lepton Yukawa couplings. At large  $t_\beta$ , the  $A/H \rightarrow \tau\tau$  provides the strongest constraints, excluding  $t_\beta \gtrsim 10$  for a large range of BSM Higgs masses. Below the top threshold,  $100 \text{ GeV} < m_H < 2m_t$ , this channel can nearly probe the entire range of  $t_\beta$ , setting the strongest constraints [23]. The exclusion region for  $\gamma\gamma$  is similar to those of the Type-I 2HDM, while the exclusion region for  $VV$ ,  $H \rightarrow hZ$  and  $H \rightarrow hh$  are reduced comparing to the left panel, given the smaller value of  $c_{\beta-\alpha}$  used here. The global fit to the LHC SM-like Higgs coupling measurements excludes  $t_\beta \lesssim 0.4$  and  $t_\beta \gtrsim 2.5$  for  $c_{\beta-\alpha} = 0.05$ .

## V. NON-DEGENERATE CASE: $H/A \rightarrow AZ/HZ$

The previous section focused on the degenerate case of  $m_H = m_A = m_{H^\pm}$ . Once there is a sizeable mass splitting between the BSM Higgs masses, additional exotic channels such as  $H/A \rightarrow AZ/HZ/H^\pm W^\mp$  will open up and quickly dominate the decay branching fractions. As a result, the reach of conventional searches shown in the last section will be reduced. At the same time, these exotic channels provide new opportunities for BSM Higgs searches at the LHC [77–82].

Under the alignment limit, the decay branching fractions of  $H/A \rightarrow AZ/HZ/H^\pm W^\mp$  are unsuppressed. The most promising final states are  $A/H \rightarrow HZ/AZ \rightarrow b\bar{b}l\bar{l}$  and  $\tau\tau l\bar{l}$ , which allow for a clean identification through the dileptons from  $Z$  decay [77, 79]. These modes have been analysed by both CMS [58, 59] and ATLAS [57], as listed in Sec. III.

In what follows, we will first present the constraints on the parameter space of  $\{t_\beta, c_{\beta-\alpha}, m_A, m_H\}$  from  $H/A \rightarrow AZ/HZ$  channel alone, focusing on the parameter dependence. We will then present  $H/A \rightarrow AZ/HZ$  together with all other direct and indirect search channels and discuss the complementarity of various channels.

### A. $m_A$ vs. $m_H$

Let us study the explicit heavy Higgs mass dependence by looking at the  $m_A$  vs.  $m_H$  plane of the 2HDM parameter space. In the top panel of Fig. 2 we show the constraints from the  $A/H \rightarrow HZ/AZ$  channel for the Type-I (left) and Type-II (right) in the alignment limit,  $c_{\beta-\alpha} = 0$ . Away from the alignment limit, these constraints are weakened given the suppressed coupling  $g_{HAZ} \propto s_{\beta-\alpha}$ . In the gap region along  $m_A \sim m_H$ , the exotic decay modes are kinematically inaccessible.

For the Type-I 2HDM with low  $t_\beta = 1.5$  (blue), the 13 TeV searches exclude parent particle masses up to 800 GeV for a daughter particle mass between 80 and 350 GeV. For higher values of  $t_\beta$ , these constraints are weakened due to the suppression of Yukawa couplings  $g_{Aff/Hff} \sim t_\beta^{-1}$  resulting in a reduced production cross section. The reach for intermediate  $t_\beta = 7$  region (red) is reduced greatly, while it vanishes for even larger values of  $t_\beta$ . The asymmetry between  $A$  and  $H$  is due to the different parent particle production cross sections as well as daughter particle decay branching ratios.

While at low  $t_\beta = 1.5$  the reach for the Type-I and Type-II 2HDM are very similar, at large  $t_\beta$  the Type-II 2HDM has an enhanced reach due to the  $t_\beta$  enhancement of bottom (and  $\tau$ ) Yukawa couplings. At  $t_\beta = 30$  (green) the  $A/H \rightarrow HZ/AZ$  search channel constrains the kinematically allowed region up to Higgs masses of  $m_{A/H} \sim 800$  GeV, with the exception of very small daughter particle masses. The constraints are weakest for intermediate values of  $t_\beta \sim 7$  case (red), with the parent particle mass excluded only up to about 700 GeV.

In the lower panels of Fig. 2 we present the global constraints on the 2HDM parameter space for  $c_{\beta-\alpha} = 0$  and  $t_\beta = 1.5$ . In particular, we show the regions excluded by Higgs searches via the  $A/H \rightarrow HZ/AZ$  (blue),  $A/H \rightarrow \tau\tau$  (orange),  $A/H \rightarrow \gamma\gamma$  (brown) and  $h \rightarrow AA/HH$  (cyan) channels as well as  $ttZ$  rate measurements (green). Furthermore we include the LEP search results (purple) and constraints arising from the measurements of the Higgs width,  $\Gamma_h \in (0.08, 9.16)$  MeV (grey). Additional constraints from the  $A \rightarrow Zh$  and  $H \rightarrow VV$ ,  $hh$  channels vanish in the alignment limit, while search results from  $A/H \rightarrow bb$ ,  $\mu\mu$  and  $tt$  are too weak to set any constraint.

For both Type-I and Type-II 2HDMs, the combination of all channels cover the majority of the region in which one of the Higgs masses is below the di-top threshold,  $m_A, m_H < 2m_t$ . In addition to  $A/H \rightarrow HZ/AZ$ , these constraints come from direct searches for the lighter BSM Higgs state which decays into conventional final states  $A/H \rightarrow \gamma\gamma$  and  $\tau\tau$ . In particular, the gap region for  $A/H \rightarrow HZ/AZ$  is mostly covered by these searches. However, these channels become inefficient for Higgs mass above  $2m_t$ , where  $A/H \rightarrow tt$  opens up. This not only decreases the branching fraction into the clean  $A/H \rightarrow \gamma\gamma$  and  $\tau\tau$  final states but it can also increase the heavy Higgs widths significantly which imposes a general

problem for resonant searches.

Interestingly, this region can be probed by the measurements of  $ttZ$  rate, which effectively constrains the process  $A/H \rightarrow HZ/AZ \rightarrow ttZ$ . Parent particle masses around 450–700 GeV and daughter particle mass around 350–450 GeV are excluded by this rate measurement. Although a resonant search would be challenging due to large Higgs widths, this result motivates a dedicated Higgs search utilizing this channel.

At very low masses,  $m_A, m_H < m_h/2$ , the BSM Higgs states can be produced in the decay of the SM Higgs  $h \rightarrow AA, HH$ . These channels have been constrained both directly in a variety of final states outlined in Sec. III and via their impact on the Higgs width itself. Both direct searches and indirect Higgs width measurements result in similar constraints in the 2HDM parameter space, excluding light masses  $m_A, m_H < m_h/2$ . Finally, searches at LEP provide additional constraints at low masses  $m_A + m_H \lesssim 200$  GeV.

### B. $\tan\beta$ vs. $\cos(\beta - \alpha)$

Let us now compare the reach of the direct BSM Higgs searches with the indirect constraints from the precision SM-like Higgs coupling measurements, which are best studied in the  $c_{\beta-\alpha}$  vs.  $t_\beta$  plane.

In Fig. 3, we show the constraints from the latest LHC Higgs coupling precision measurements as the grey shaded region for both Type-I (left) and Type-II (right) 2HDMs. The central region around the alignment limit of  $c_{\beta-\alpha} = 0$  is always unconstrained by the Higgs coupling measurements. For the Type-I 2HDM, the fermion Yukawa couplings can be written as  $g_{hff} = s_{\beta-\alpha} + c_{\beta-\alpha}/t_\beta$ . At low  $t_\beta$ , even small deviations from the alignment limit results in an enhanced Higgs production rate and decay width into bottom/tau pairs which can be excluded by Higgs couplings measurements. For large values of  $t_\beta$ , the Yukawa couplings are almost  $t_\beta$ -independent,  $g_{hff} \sim s_{\beta-\alpha}$ , resulting in weaker constraints of  $|c_{\beta-\alpha}| < 0.35$ , mainly from the measurement of the vector boson couplings  $g_{hZZ}$ .

For the Type-II 2HDM, both the small and large  $t_\beta$  region are tightly constrained by fermion Yukawa couplings. Away from the alignment limit, the SM-like Higgs production rate in gluon-gluon fusion quickly increases as low  $t_\beta$ , while the Higgs decay widths into bottom and tau pairs are enhanced at high  $t_\beta$ . The bounds are weakest for intermediate values of  $t_\beta \sim 1$ , constraining  $|c_{\beta-\alpha}| < 0.08$ . Once loop contributions from heavy Higgses are included, the shape of the allowed region will be tilted, with tighter constraints at the large  $t_\beta$  region for the Type-I 2HDM, as shown in Refs. [6–8]. For the Type-II 2HDM, there is an additional allowed wrong-sign Yukawa “arm” region [7, 83–85] for  $0.1 < c_{\beta-\alpha} < 0.5$  and  $t_\beta > 4$ .

The upper panels of Fig. 3 also show the bounds obtained from the exotic Higgs decay searches for  $A \rightarrow$

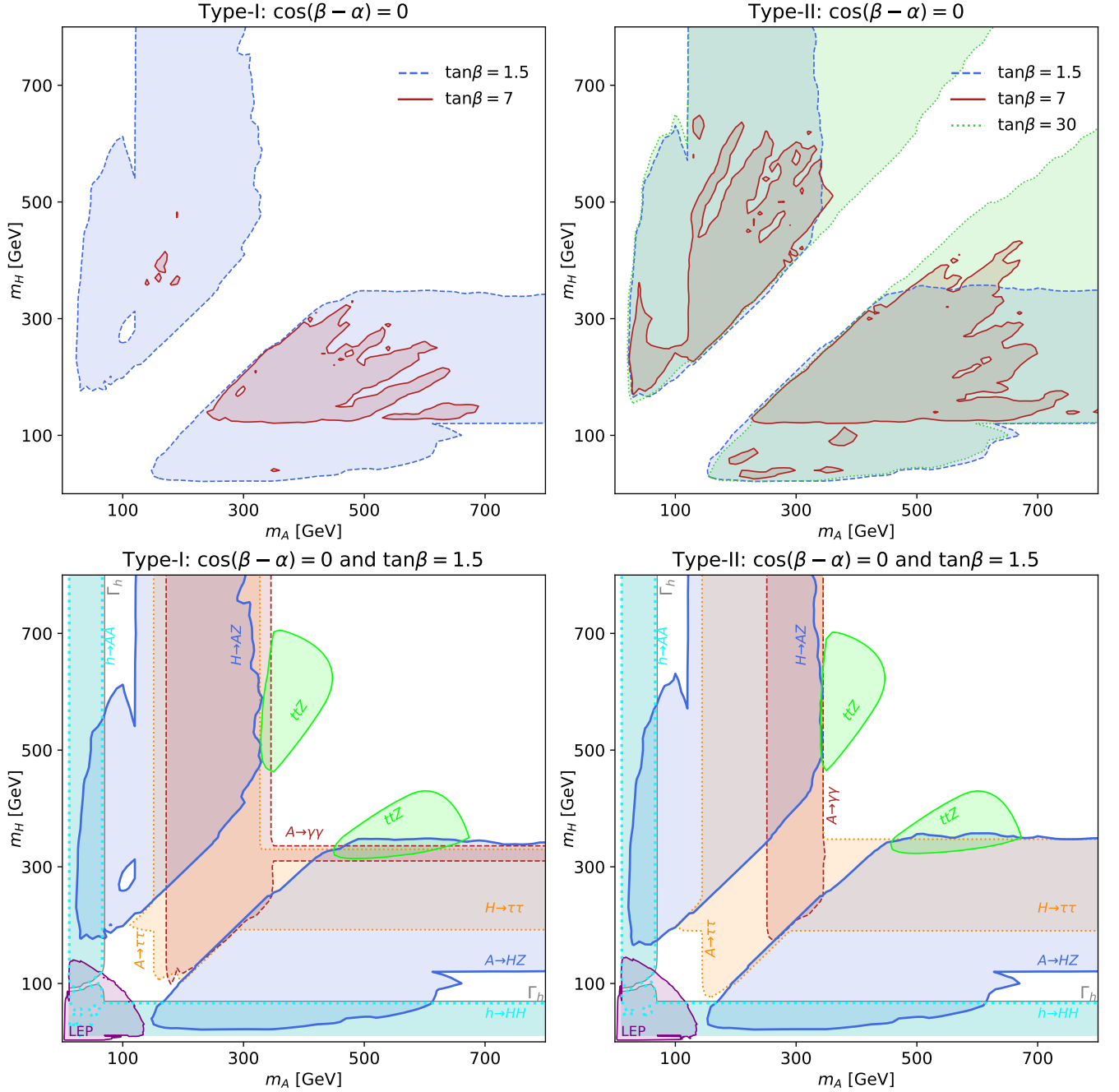


FIG. 2. Constraints on the Type-I (left panel) and the Type-II (right panel) 2HDM in  $m_A$  vs.  $m_H$  plane. **Top:** Parameter space excluded at 95% C.L. by the  $A/H \rightarrow HZ/AZ$  search in the alignment limit,  $c_{\beta-\alpha} = 0$ , for  $t_\beta = 1.5$  (blue), 7 (red) and 30 (green). **Bottom:** Constraints at 95% C.L. for  $c_{\beta-\alpha} = 0$  and  $t_\beta = 1.5$  from LHC searches for  $A/H \rightarrow HZ/AZ$  (blue),  $A/H \rightarrow \tau\tau$  (dotted orange),  $A/H \rightarrow \gamma\gamma$  (dashed brown),  $h \rightarrow AA/HH$  (dotted cyan) and  $ttZ$  production (green) as well as LEP searches (purple) and the Higgs width measurement  $\Gamma_h \in (0.08, 9.16)$  MeV (grey).

$HZ \rightarrow b\bar{b}l\bar{l}/\tau\tau l\bar{l}$  for fixed  $m_A = 400$  GeV and for  $m_H = 50$  GeV (red),  $m_H = 150$  GeV (blue) and  $m_H = 250$  GeV (green). For the Type-I 2HDM (left), small  $t_\beta \lesssim 5$  region is excluded. For  $m_H = 50$  GeV, the bounds are almost independent of  $c_{\beta-\alpha}$ , with the exception of a small band around  $g_{Hff} = c_{\beta-\alpha} - s_{\beta-\alpha}/t_\beta = 0$ , where the decay  $H \rightarrow b\bar{b}/\tau\tau$  is suppressed and the sen-

sitivity vanishes. For larger daughter masses, the sensitivity decreases away from the alignment limit, since the  $H \rightarrow b\bar{b}/\tau\tau$  branching fraction is reduced both due to the suppression around  $g_{Hff} = 0$  and the increasing decay branching fractions for the competing  $H \rightarrow VV$  and  $hZ$  channels at large  $|c_{\beta-\alpha}|$ . The later is particularly important for heavy Higgs  $m_H > 2m_W$ , where the

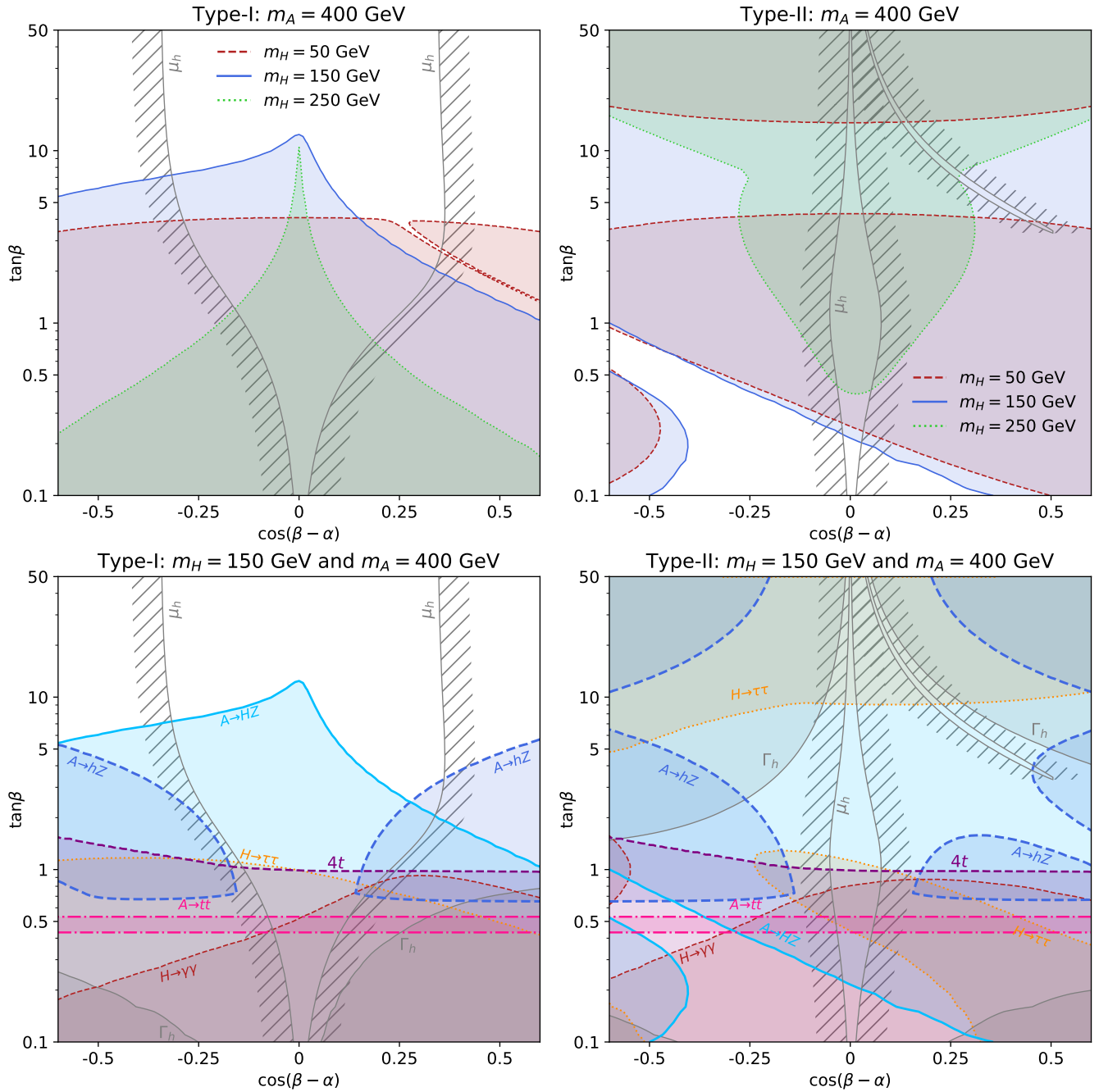


FIG. 3. Constraints on the Type-I (left panel) and the Type-II (right panel) 2HDM in  $t_\beta - c_{\beta-\alpha}$  plane. **Top:** Parameter space excluded at 95% C.L. by the  $A/H \rightarrow HZ/AZ$  search for  $m_A = 400$  GeV and  $m_H = 50$  GeV (red), 150 GeV (blue) and 250 GeV (green), and by the global fit of SM-like Higgs couplings strength  $\mu_h$  (grey). **Bottom:** Constraints at 95% C.L. for  $m_A = 400$  GeV and  $m_H = 150$  GeV from LHC searches for  $A \rightarrow HZ$  (blue),  $A \rightarrow hZ$  (dashed dark blue),  $H \rightarrow \tau\tau$  (dotted orange),  $H \rightarrow \gamma\gamma$  (dashed brown),  $A \rightarrow tt$  (dot-dashed magenta) and  $4t$  production (dashed purple) as well as the global fit of SM-like Higgs couplings strength  $\mu_h$  (grey hatched region).

sensitivity sharply peaks around the alignment limit, as can be seen from the green curve for  $m_H = 200$  GeV.

The Type-II 2HDM (right panel), on the other hand, also receives constraints at large  $t_\beta$  due to the enhanced bottom-associated Higgs production mode. For  $m_H = 50$  and 250 GeV, one can identify two distinct regions cor-

responding to  $bbA$  associated production at high  $t_\beta \gtrsim 10$  and the gluon fusion at low  $t_\beta \lesssim 10$ , while for  $m_H = 150$  both these regions overlap, covering the entire parameter space. As for Type-I, the sensitivity decreases for large  $|c_{\beta-\alpha}|$  due to the competing  $H \rightarrow VV$  and  $hZ$  channels, which is especially visible for  $m_H = 250$  GeV. A band

with no sensitivity is now visible around  $g_{Hbb} = g_{H\tau\tau} = c_{\beta-\alpha} + s_{\beta-\alpha}t_\beta = 0$  as a result of the cancellation between the first and second term.

The lower panels of Fig. 3 show the complementary between the Higgs couplings precision measurements (grey hatched region) and the direct exclusion limits from various BSM Higgs search channels for  $m_A = 400$  GeV and  $m_H = 150$  GeV. The leading constraints come from the heavy CP-even Higgs decay  $H \rightarrow \tau\tau$  and  $\gamma\gamma$ , the CP-odd Higgs decay  $A \rightarrow tt$  and  $hZ$ , as well as the  $4t$  cross section measurement. We do not show additional constraints from the  $H/A \rightarrow VV, hh, \mu\mu$  and  $bb$  channels, which are generally weaker.

For Type-I, the  $H \rightarrow \tau\tau$  and  $\gamma\gamma$  channel constrain  $t_\beta < 1$  with a  $c_{\beta-\alpha}$  dependence entering both in the production and decay. The  $A \rightarrow tt$  constraints are independent of  $c_{\beta-\alpha}$  and limited by a suppressed production rate towards larger  $t_\beta$  and a large decay width  $\Gamma_A > 0.2m_A$  at low  $t_\beta$ . The  $A \rightarrow hZ$  channel constrains  $|c_{\beta-\alpha}| > 0.2$  for  $0.8 \lesssim t_\beta \lesssim 5$ , where the low  $t_\beta$  limit is again due to a large width  $\Gamma_A$ , limiting the applicability of the resonance search. Finally the  $4t$  cross section measurement can constrain the  $t_\beta \lesssim 1$  region, with the limits constraining the (offshell)  $ttH$  production at negative  $c_{\beta-\alpha}$  and  $ttA$  production positive  $c_{\beta-\alpha}$ , resulting in  $c_{\beta-\alpha}$ -dependent and  $c_{\beta-\alpha}$ -independent bounds, respectively.

For Type-II, the additional  $bbA/bbH$  production modes result in additional constraints from  $H \rightarrow \tau\tau$  and  $A \rightarrow hZ$  at high  $t_\beta > 10$ . Additionally, the  $H \rightarrow \tau\tau$  reach is reduced at low  $t_\beta < 1$  for negative  $c_{\beta-\alpha}$  where the  $g_{H\tau\tau} = c_{\beta-\alpha} + s_{\beta-\alpha}t_\beta$  coupling vanishes. Also note the exclusion region of  $A \rightarrow hZ$  for  $c_{\beta-\alpha} > 0$  and intermediate  $t_\beta \sim 2$  is split in two parts, due to the vanishing branching fraction for  $h \rightarrow bb$  when  $g_{hbb} = s_{\beta-\alpha} - c_{\beta-\alpha}t_\beta = 0$ .

Combining all constraints, we can see that the Higgs precision measurements exclude large deviations away from the alignment limit, while the direct BSM Higgs searches provide additional constraints also in the alignment limit. In particular, the exotic Higgs decay  $A \rightarrow HZ$  provides important constraints for intermediate values of  $t_\beta$ , showing its complementarity to the conventional searches.

### C. $\tan\beta$ vs. $m_A$

While in Fig. 1, we have considered the constraints in the  $m_A$  vs.  $t_\beta$  plane for a degenerate mass spectrum, we now consider the same parameter space again for a non-degenerate spectrum permitting the exotic decay channel  $A/H \rightarrow HZ/AZ$ .

The top panel of Fig. 4 shows the constraints from the  $A/H \rightarrow HZ/AZ$  channel for Type-I (left panel) and the Type-II (right panel) 2HDM for  $m_H = 200$  GeV. The low mass region  $m_A < m_H - m_Z = 110$  GeV probes the decay  $H \rightarrow AZ$  while the high mass region  $m_A > m_H + m_Z = 290$  GeV is sensitive to decay  $A \rightarrow HZ$ .

The largest reach is obtained under the alignment limit of  $c_{\beta-\alpha} = 0$ . For the Type-I 2HDM,  $t_\beta$  up to about 10 can be excluded for  $m_A > 290$  GeV, while the reach in  $t_\beta$  is reduced when  $c_{\beta-\alpha}$  increases. For small  $m_A$ , when  $H \rightarrow AZ$  is kinematically accessible,  $t_\beta \lesssim 2$  can be excluded. Regions with large  $t_\beta$  remain unconstrained, given the suppression of all the Yukawa couplings.

For the Type-II 2HDM, the reach extends to large  $t_\beta$  where the  $bbA/H$  production rate is enhanced. Almost the entire range of  $t_\beta$  is constrained by the  $A/H \rightarrow HZ/AZ$  channel with the exceptions of the low  $t_\beta < 0.2$  region, where the branching fractions for  $H/A \rightarrow bb$  and  $\tau\tau$  are suppressed, and a gap at intermediate  $t_\beta \sim 5$  at low and high masses  $m_A$ , where the Higgs production cross section is reduced.

The lower panels of Fig. 4 present the global constraints from direct search channels of the BSM Higgses, the Higgs coupling  $\mu_h$  and Higgs width  $\Gamma_h$  precision measurements, and the  $4t$  cross section measurements. While for  $m_A \lesssim 300$  GeV, the strongest conventional search constraints are related to the decay of the pseudoscalar  $A$ , at large  $m_A \gtrsim 300$  GeV constraints mainly come from direct searches for  $H$ , whose mass is fixed to  $m_H = 200$  GeV. Therefore, there is no dependence on  $m_A$  for the  $\tau\tau$ ,  $\gamma\gamma$  and  $4t$  exclusion limits in the large  $m_A$  region.

For the Type-I 2HDM with  $c_{\beta-\alpha} = 0.1$ , the small  $m_A < m_h/2$  and the small  $t_\beta \lesssim 2 - 3$  are excluded combining all channels, with the  $A \rightarrow HZ$  gap of  $|m_A - m_H| < m_Z$  region completely covered by the  $A/H \rightarrow \tau\tau$  and  $\gamma\gamma$ , the  $4t$ , and the  $A \rightarrow hZ$  channels. For the Type-II 2HDM with  $c_{\beta-\alpha} = 0.05$ , the small  $t_\beta \lesssim 1$  region is covered mostly by the  $H/A \rightarrow \gamma\gamma$ , the  $4t$ , and the  $A \rightarrow HZ$  and  $hZ$  channels, while large  $t_\beta$  region is covered by  $H/A \rightarrow \tau\tau$  and  $A \rightarrow HZ$ . Note again that we have fixed  $m_H = 200$  GeV, which causes the  $H \rightarrow \tau\tau$  channel to exclude the entire  $t_\beta$  range for  $m_A \gtrsim 100$  GeV. Combinations of all channels exclude nearly the entire parameter space except for intermediate  $t_\beta \sim 2$  with  $m_A \sim 100$  GeV.

## VI. CONCLUSION AND OUTLOOK

Since the discovery of 125 GeV Higgs boson, there have been many theoretical and experimental studies searching for additional scalar particles. In the framework of the 2HDM, besides the usual search methods for the non-SM Higgs bosons, such as SM Higgs precision measurements, conventional Higgs decays channels ( $A/H \rightarrow f\bar{f}, VV, \gamma\gamma$ ), and decay to SM Higgs ( $H \rightarrow hh, A \rightarrow hZ$ ), exotic decays of BSM Higgses such as  $A/H \rightarrow HZ/AZ$  offer additional discovery potential when such modes are kinematically open. On the one hand, existing constraints based on the conventional searches will be relaxed given the reduced decay branching fractions. On the other hand, such exotic decay modes provide additional search channels in the parameter regions with large

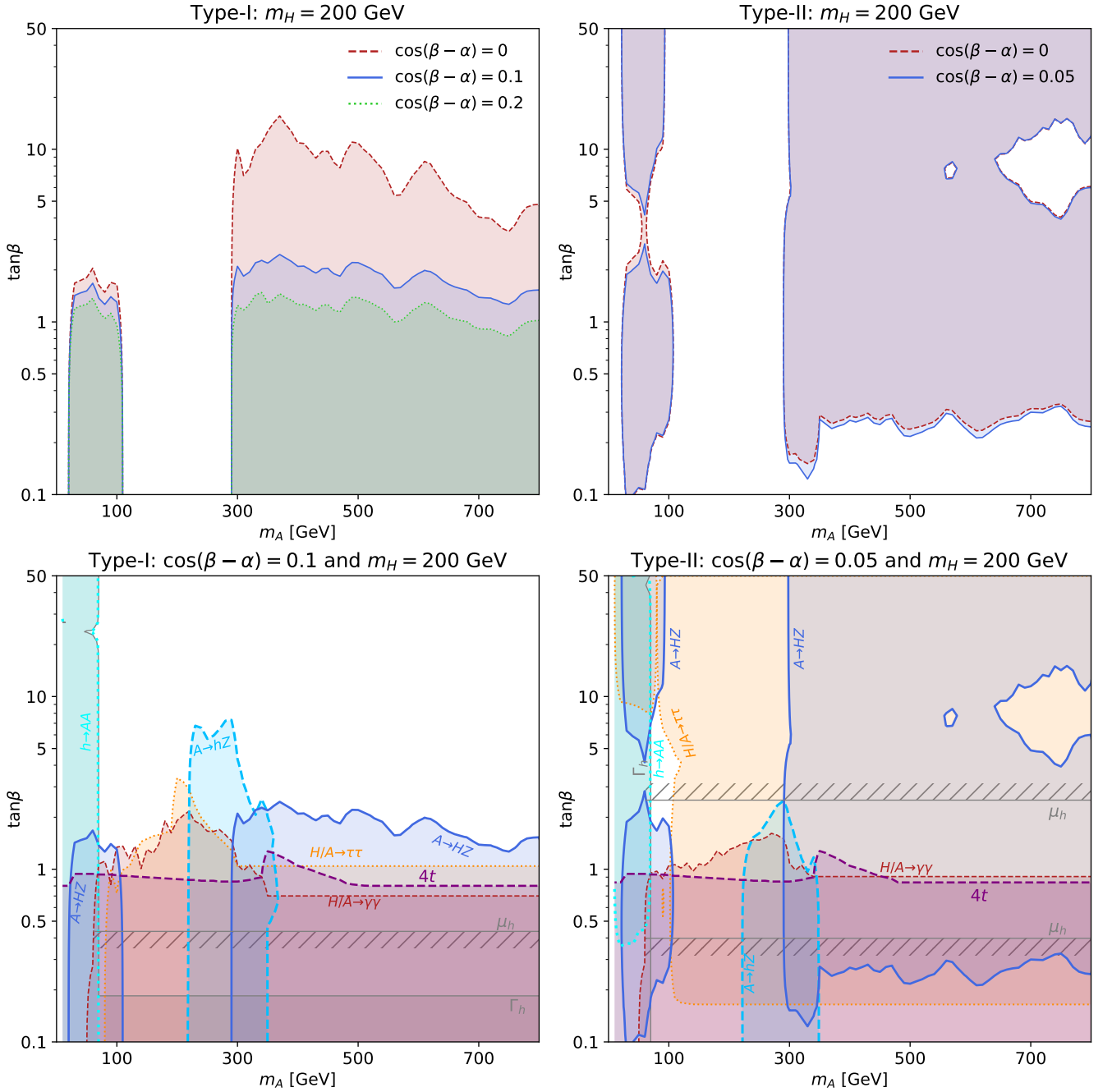


FIG. 4. Constraints on the Type-I (left panel) and the Type-II (right panel) 2HDM in  $m_A - t_\beta$  plane. **Top:** Parameter space excluded at 95% C.L. by the  $A/H \rightarrow HZ/AZ$  search for  $m_H = 200$  GeV and  $c_{\beta-\alpha} = 0$  (red), 0.1 (blue) and 0.2 (green) in the left panel and  $c_{\beta-\alpha} = 0$  (red) and 0.05 (blue) in the right panel. **Bottom:** Constraints at 95% C.L. for  $m_H = 200$  GeV and  $c_{\beta-\alpha} = 0.1$  from LHC searches for  $A \rightarrow HZ$  (blue),  $A \rightarrow hZ$  (dashed dark blue),  $H \rightarrow AA$  (dashed cyan),  $H/A \rightarrow \tau\tau$  (dotted orange),  $H/A \rightarrow \gamma\gamma$  (dashed brown) and  $4t$  production (dashed magenta) as well as the global fit of SM-like Higgs couplings strength  $\mu_h$  (grey hatched region) and the Higgs width measurement  $\Gamma_h \notin (0.08, 9.16)$  MeV (grey).

mass splittings between non-SM Higgses.

In this study, we focused on the exotic decay of  $A/H \rightarrow HZ/AZ$ , which is the most promising channel given the large branching fraction as well as the clean experimental signal of  $b\bar{b}l\bar{l}$  and  $\tau\bar{\tau}l\bar{l}$ . ATLAS [57] and CMS [58, 59] have performed searches for these decay channels at both

8 TeV and 13 TeV. We performed a comprehensive study of the BSM neutral Higgses in the Type-I and Type-II 2HDMs under existing direct and indirect search results, and studied the constraints on their parameter spaces. We list our main findings below.

- Given the theoretical considerations and electroweak

precision measurements, large mass splittings  $\gtrsim 200$  GeV in BSM Higgs masses in the 2HDMs are generally not allowed for large BSM Higgs masses  $\gtrsim 1$  TeV [13]. Therefore, the LHC is the most relevant machine to probe the parameter space of non-degenerate 2HDMs. While the  $bb\ell\ell$  final state is used in the current 13 TeV searches, final state with  $\tau\tau\ell\ell$  will be promising at high luminosity given the reduced SM backgrounds comparing to the  $bb\ell\ell$  mode.

- For the conventional search channels, the most sensitive ones are  $H/A \rightarrow \tau\tau$  and  $\gamma\gamma$ . Other channels only provide subdominant constraints.
- The low mass region of  $m_{A/H} \sim 100$  GeV is still challenging for both the conventional and exotic decay channels, motivating a continuation of searches in this mass region. For even lower masses of  $m_{A/H} < m_h/2$ , both the SM-like Higgs width measurements and  $h \rightarrow AA/HH$  can be used to constrain this parameter region. In particular,  $h \rightarrow AA$  is unsuppressed even under the alignment limit.
- Other than the resonant searches for the BSM Higgses, rate measurements of SM processes, for example,  $4t$  or  $ttZ$ , can be used to constrain  $ttH/ttA$  or  $HZ/AZ$  production. It is especially useful in the high mass region above the  $t\bar{t}$  threshold when the decay widths of  $H$  and  $A$  are large and the resonant searches are ineffective. In particular, the usefulness of  $ttZ$  channel motivates a dedicated search for  $A \rightarrow HZ \rightarrow ttZ$  in the future.
- Combing all the searches, for the Type-I 2HDM, most of the  $m_{A,H} < 350$  GeV regions are excluded for low  $\tan\beta$  under the alignment case. Limits are reduced at intermediate and large  $\tan\beta$  as well as  $c_{\beta-\alpha} \neq 0$ . For the Type-II 2HDM, the limits for large  $\tan\beta$  are

stronger, given the enhanced production cross sections.

- The exotic decays modes, which have enhanced reach under the alignment limit, show great complementarity with the SM-like Higgs precision measurements, as well as the direct search modes of  $VV$ ,  $hZ$  and  $hh$ , which has reduced sensitivity near the alignment region.
- The exotic decay mode of  $A \rightarrow HZ$  extends the reach in  $m_A$  and  $\tan\beta$  beyond the conventional search channels. Combining all the LHC search channels for the non-SM Higgses, for  $m_H = 200$  GeV, the entire region of  $m_A$  up to about 800 GeV are excluded in the Type-I 2HDM for the low  $\tan\beta$ . Almost the entire region of  $m_A$  vs.  $\tan\beta$  plane is excluded for the Type-II 2HDM except for a small region around  $\tan\beta \sim 2$  and  $m_A \sim 100$  GeV.

Besides minimal realizations of the 2HDM that we focused on in this paper, the exotic decay channel  $A/H \rightarrow HZ/AZ$  channel has also been proven to be a useful probe for CPV realizations [86] and singlet extension [87–90] of the 2HDM. Additionally, other exotic decay modes besides  $A/H \rightarrow HZ/AZ$ , such as  $H^\pm \rightarrow AW, HW$ ,  $A/H \rightarrow H^\pm W^\mp$ , could also extend the reach beyond the direct search via conventional decay channels, and indirect reach via Higgs precision measurements, especially at 100 TeV  $pp$  colliders [82]. Combing all the search channels will provide valuable information towards Higgs sectors beyond the SM.

## ACKNOWLEDGMENTS

WS is supported by the Australian Research Council Discovery Project DP180102209. FK is supported by the Department of Energy under Grant DE-AC02-76SF00515. SS is supported by the Department of Energy under Grant DE-SC0009913.

- 
- [1] **ATLAS** Collaboration, G. Aad *et al.*, “Observation of a new particle in the search for the Standard Model Higgs boson with the ATLAS detector at the LHC,” *Phys. Lett. B* **716** (2012) 1–29, [arXiv:1207.7214 \[hep-ex\]](#).
- [2] **CMS** Collaboration, S. Chatrchyan *et al.*, “Observation of a new boson at a mass of 125 GeV with the CMS experiment at the LHC,” *Phys. Lett. B* **716** (2012) 30–61, [arXiv:1207.7235 \[hep-ex\]](#).
- [3] G. C. Branco, P. M. Ferreira, L. Lavoura, M. N. Rebelo, M. Sher, and J. P. Silva, “Theory and phenomenology of two-Higgs-doublet models,” *Phys. Rept.* **516** (2012) 1–102, [arXiv:1106.0034 \[hep-ph\]](#).
- [4] **ATLAS** Collaboration, T. A. collaboration, “Combined measurements of Higgs boson production and decay using up to 80 fb<sup>-1</sup> of proton–proton collision data at  $\sqrt{s} = 13$  TeV collected with the ATLAS experiment,”
- [5] **LHC Higgs Cross Section Working Group** Collaboration, J. R. Andersen *et al.*, “Handbook of LHC Higgs Cross Sections: 3. Higgs Properties,” [arXiv:1307.1347 \[hep-ph\]](#).
- [6] N. Chen, T. Han, S. Su, W. Su, and Y. Wu, “Type-II 2HDM under the Precision Measurements at the  $Z$ -pole and a Higgs Factory,” *JHEP* **03** (2019) 023, [arXiv:1808.02037 \[hep-ph\]](#).
- [7] J. Gu, H. Li, Z. Liu, S. Su, and W. Su, “Learning from Higgs Physics at Future Higgs Factories,” *JHEP* **12** (2017) 153, [arXiv:1709.06103 \[hep-ph\]](#).
- [8] N. Chen, T. Han, S. Li, S. Su, W. Su, and Y. Wu, “Type-I 2HDM under the Higgs and Electroweak Precision Measurements,” [arXiv:1912.01431](#)

- [hep-ph].
- [9] N. Chen, T. Han, S. Su, W. Su, and Y. Wu, “Implication of Higgs Precision Measurement on New Physics,” in *International Workshop on Future Linear Colliders (LCWS 2018) Arlington, Texas, USA, October 22-26, 2018*. 2019. [arXiv:1901.09067 \[hep-ph\]](#).
- [10] N. Chen, J. Gu, T. Han, H. Li, Z. Liu, H. Song, S. Su, W. Su, Y. Wu, and J. M. Yang, “New physics implication of Higgs precision measurements New physics implication of Higgs precision measurements,” *Int. J. Mod. Phys. A* **34** (2019) no. 13n14, 1940012, [arXiv:1808.10177 \[hep-ph\]](#).
- [11] W. Su, M. White, A. G. Williams, and Y. Wu, “Exploring the low  $\tan\beta$  region of two Higgs doublet models at the LHC,” [arXiv:1909.09035 \[hep-ph\]](#).
- [12] F. Kling, *Exotic Higgs Decays*. PhD thesis, Arizona U., 2016-07-06. <http://arizona.openrepository.com/arizona/handle/10150/620861>.
- [13] F. Kling, J. M. No, and S. Su, “Anatomy of Exotic Higgs Decays in 2HDM,” *JHEP* **09** (2016) 093, [arXiv:1604.01406 \[hep-ph\]](#).
- [14] B. Coleppa, F. Kling, and S. Su, “Constraining Type II 2HDM in Light of LHC Higgs Searches,” *JHEP* **01** (2014) 161, [arXiv:1305.0002 \[hep-ph\]](#).
- [15] CMS Collaboration, C. Collaboration, “Combined measurements of the Higgs boson’s couplings at  $\sqrt{s} = 13$  TeV,”.
- [16] CMS Collaboration, A. M. Sirunyan *et al.*, “Measurements of the Higgs boson width and anomalous  $HVV$  couplings from on-shell and off-shell production in the four-lepton final state,” *Phys. Rev. D* **99** (2019) no. 11, 112003, [arXiv:1901.00174 \[hep-ex\]](#).
- [17] CMS Collaboration, A. M. Sirunyan *et al.*, “Search for MSSM Higgs bosons decaying to  $\mu^+\mu^-$  in proton-proton collisions at  $\sqrt{s} = 13$  TeV Search for MSSM Higgs bosons decaying to  $\mu^+\mu^-$  in proton-proton collisions at  $\sqrt{s} = 13$  TeV,” *Phys. Lett. B* **798** (2019) 134992, [arXiv:1907.03152 \[hep-ex\]](#).
- [18] ATLAS Collaboration, M. Aaboud *et al.*, “Search for scalar resonances decaying into  $\mu^+\mu^-$  in events with and without  $b$ -tagged jets produced in proton-proton collisions at  $\sqrt{s} = 13$  TeV with the ATLAS detector,” *JHEP* **07** (2019) 117, [arXiv:1901.08144 \[hep-ex\]](#).
- [19] CMS Collaboration, A. M. Sirunyan *et al.*, “Search for beyond the standard model Higgs bosons decaying into a  $b\bar{b}$  pair in  $pp$  collisions at  $\sqrt{s} = 13$  TeV,” *JHEP* **08** (2018) 113, [arXiv:1805.12191 \[hep-ex\]](#).
- [20] ATLAS Collaboration, G. Aad *et al.*, “Search for heavy neutral Higgs bosons produced in association with  $b$ -quarks and decaying to  $b$ -quarks at  $\sqrt{s} = 13$  TeV with the ATLAS detector,” [arXiv:1907.02749 \[hep-ex\]](#).
- [21] CMS Collaboration, A. M. Sirunyan *et al.*, “Search for additional neutral MSSM Higgs bosons in the  $\tau\tau$  final state in proton-proton collisions at  $\sqrt{s} = 13$  TeV,” *JHEP* **09** (2018) 007, [arXiv:1803.06553 \[hep-ex\]](#).
- [22] CMS Collaboration, A. M. Sirunyan *et al.*, “Search for a low-mass  $\tau^+\tau^-$  resonance in association with a bottom quark in proton-proton collisions at  $\sqrt{s} = 13$  TeV,” *JHEP* **05** (2019) 210, [arXiv:1903.10228 \[hep-ex\]](#).
- [23] ATLAS Collaboration, G. Aad *et al.*, “Search for heavy Higgs bosons decaying into two tau leptons with the ATLAS detector using  $pp$  collisions at  $\sqrt{s} = 13$  TeV,” [arXiv:2002.12223 \[hep-ex\]](#).
- [24] CMS Collaboration, A. M. Sirunyan *et al.*, “Search for a standard model-like Higgs boson in the mass range between 70 and 110 GeV in the diphoton final state in proton-proton collisions at  $\sqrt{s} = 8$  and 13 TeV,” *Phys. Lett. B* **793** (2019) 320–347, [arXiv:1811.08459 \[hep-ex\]](#).
- [25] CMS Collaboration, A. M. Sirunyan *et al.*, “Search for physics beyond the standard model in high-mass diphoton events from proton-proton collisions at  $\sqrt{s} = 13$  TeV,” *Phys. Rev. D* **98** (2018) no. 9, 092001, [arXiv:1809.00327 \[hep-ex\]](#).
- [26] ATLAS Collaboration, G. Aad *et al.*, “Search for Scalar Diphoton Resonances in the Mass Range 65 – 600 GeV with the ATLAS Detector in  $pp$  Collision Data at  $\sqrt{s} = 8$  TeV,” *Phys. Rev. Lett.* **113** (2014) no. 17, 171801, [arXiv:1407.6583 \[hep-ex\]](#).
- [27] ATLAS Collaboration, M. Aaboud *et al.*, “Search for new phenomena in high-mass diphoton final states using 37  $\text{fb}^{-1}$  of proton–proton collisions collected at  $\sqrt{s} = 13$  TeV with the ATLAS detector,” *Phys. Lett. B* **775** (2017) 105–125, [arXiv:1707.04147 \[hep-ex\]](#).
- [28] ATLAS Collaboration, T. A. collaboration, “Search for resonances in the 65 to 110 GeV diphoton invariant mass range using 80  $\text{fb}^{-1}$  of  $pp$  collisions collected at  $\sqrt{s} = 13$  TeV with the ATLAS detector,”.
- [29] CMS Collaboration, A. M. Sirunyan *et al.*, “Search for heavy Higgs bosons decaying to a top quark pair in proton-proton collisions at  $\sqrt{s} = 13$  TeV,” [arXiv:1908.01115 \[hep-ex\]](#).
- [30] CMS Collaboration, A. M. Sirunyan *et al.*, “Search for a new scalar resonance decaying to a pair of Z bosons in proton-proton collisions at  $\sqrt{s} = 13$  TeV,” *JHEP* **06** (2018) 127, [arXiv:1804.01939 \[hep-ex\]](#). [Erratum: *JHEP*03,128(2019)].
- [31] ATLAS Collaboration, M. Aaboud *et al.*, “Search for heavy ZZ resonances in the  $\ell^+\ell^-\ell^+\ell^-$  and  $\ell^+\ell^-\nu\bar{\nu}$  final states using proton–proton collisions at  $\sqrt{s} = 13$  TeV with the ATLAS detector,” *Eur. Phys. J. C* **78** (2018) no. 4, 293, [arXiv:1712.06386 \[hep-ex\]](#).
- [32] CMS Collaboration, A. M. Sirunyan *et al.*, “Search for a heavy Higgs boson decaying to a pair of W bosons in proton-proton collisions at  $\sqrt{s} = 13$  TeV,” [arXiv:1912.01594 \[hep-ex\]](#).
- [33] ATLAS Collaboration, M. Aaboud *et al.*, “Search for heavy resonances decaying into  $WW$  in the  $e\nu\mu\nu$  final state in  $pp$  collisions at  $\sqrt{s} = 13$  TeV with the ATLAS detector,” *Eur. Phys. J. C* **78** (2018) no. 1, 24, [arXiv:1710.01123 \[hep-ex\]](#).
- [34] CMS Collaboration, C. Collaboration, “Summary results of high mass BSM Higgs searches using CMS run-I data,”.
- [35] ATLAS Collaboration Collaboration, “HBSM working group hMSSM summary plots,” Tech. Rep. ATL-PHYS-PUB-2019-034, CERN, Geneva, Sep, 2019. <http://cds.cern.ch/record/2689745>.
- [36] CMS Collaboration, V. Khachatryan *et al.*, “Search for a pseudoscalar boson decaying into a Z boson and the 125 GeV Higgs boson in  $l\bar{l}b\bar{b}$  final states,” *Phys. Lett. B* **748** (2015) 221–243, [arXiv:1504.04710 \[hep-ex\]](#).
- [37] CMS Collaboration, A. M. Sirunyan *et al.*, “Search for a heavy pseudoscalar boson decaying to a Z and a Higgs boson at  $\sqrt{s} = 13$  TeV,” *Eur. Phys. J. C* **79** (2019) no. 7, 564, [arXiv:1903.00941 \[hep-ex\]](#).

- [38] **ATLAS** Collaboration, G. Aad *et al.*, “Search for a CP-odd Higgs boson decaying to Zh in pp collisions at  $\sqrt{s} = 8$  TeV with the ATLAS detector,” *Phys. Lett. B* **744** (2015) 163–183, [arXiv:1502.04478 \[hep-ex\]](#).
- [39] **ATLAS** Collaboration, M. Aaboud *et al.*, “Search for heavy resonances decaying into a W or Z boson and a Higgs boson in final states with leptons and b-jets in 36 fb<sup>-1</sup> of  $\sqrt{s} = 13$  TeV pp collisions with the ATLAS detector,” *JHEP* **03** (2018) 174, [arXiv:1712.06518 \[hep-ex\]](#). [Erratum: *JHEP*11,051(2018)].
- [40] **CMS** Collaboration, V. Khachatryan *et al.*, “Searches for a heavy scalar boson H decaying to a pair of 125 GeV Higgs bosons hh or for a heavy pseudoscalar boson A decaying to Zh, in the final states with  $h \rightarrow \tau\tau$ ,” *Phys. Lett. B* **755** (2016) 217–244, [arXiv:1510.01181 \[hep-ex\]](#).
- [41] **CMS** Collaboration, A. M. Sirunyan *et al.*, “Search for a heavy pseudoscalar Higgs boson decaying into a 125 GeV Higgs boson and a Z boson in final states with two tau and two light leptons at  $\sqrt{s} = 13$  TeV,” [arXiv:1910.11634 \[hep-ex\]](#).
- [42] **CMS** Collaboration, A. M. Sirunyan *et al.*, “Search for Higgs boson pair production in the  $b\bar{b}\tau\tau$  final state in proton-proton collisions at  $\sqrt{s} = 8$  TeV,” *Phys. Rev. D* **96** (2017) no. 7, 072004, [arXiv:1707.00350 \[hep-ex\]](#).
- [43] **CMS** Collaboration, A. M. Sirunyan *et al.*, “Combination of searches for Higgs boson pair production in proton-proton collisions at  $\sqrt{s} = 13$  TeV,” *Phys. Rev. Lett.* **122** (2019) no. 12, 121803, [arXiv:1811.09689 \[hep-ex\]](#).
- [44] **ATLAS** Collaboration, G. Aad *et al.*, “Searches for Higgs boson pair production in the  $hh \rightarrow b\bar{b}\tau\tau, \gamma\gamma WW^*, \gamma\gamma bb, bbbb$  channels with the ATLAS detector,” *Phys. Rev. D* **92** (2015) 092004, [arXiv:1509.04670 \[hep-ex\]](#).
- [45] **ATLAS** Collaboration, G. Aad *et al.*, “Combination of searches for Higgs boson pairs in pp collisions at  $\sqrt{s} = 13$  TeV with the ATLAS detector,” [arXiv:1906.02025 \[hep-ex\]](#).
- [46] **ATLAS** Collaboration, M. Aaboud *et al.*, “Search for the Higgs boson produced in association with a vector boson and decaying into two spin-zero particles in the  $H \rightarrow aa \rightarrow 4b$  channel in pp collisions at  $\sqrt{s} = 13$  TeV with the ATLAS detector,” *JHEP* **10** (2018) 031, [arXiv:1806.07355 \[hep-ex\]](#).
- [47] **CMS** Collaboration, A. M. Sirunyan *et al.*, “Search for an exotic decay of the Higgs boson to a pair of light pseudoscalars in the final state with two b quarks and two  $\tau$  leptons in proton-proton collisions at  $\sqrt{s} = 13$  TeV,” *Phys. Lett. B* **785** (2018) 462, [arXiv:1805.10191 \[hep-ex\]](#).
- [48] **ATLAS** Collaboration, M. Aaboud *et al.*, “Search for Higgs boson decays into a pair of light bosons in the  $b\bar{b}\mu\mu$  final state in pp collision at  $\sqrt{s} = 13$  TeV with the ATLAS detector,” *Phys. Lett. B* **790** (2019) 1–21, [arXiv:1807.00539 \[hep-ex\]](#).
- [49] **CMS** Collaboration, A. M. Sirunyan *et al.*, “Search for an exotic decay of the Higgs boson to a pair of light pseudoscalars in the final state with two muons and two b quarks in pp collisions at 13 TeV,” *Phys. Lett. B* **795** (2019) 398–423, [arXiv:1812.06359 \[hep-ex\]](#).
- [50] **CMS** Collaboration, A. M. Sirunyan *et al.*, “Search for light pseudoscalar boson pairs produced from decays of the 125 GeV Higgs boson in final states with two muons and two nearby tracks in pp collisions at  $\sqrt{s} = 13$  TeV,” [arXiv:1907.07235 \[hep-ex\]](#).
- [51] **ATLAS** Collaboration, G. Aad *et al.*, “Search for Higgs bosons decaying to  $aa$  in the  $\mu\mu\tau\tau$  final state in pp collisions at  $\sqrt{s} = 8$  TeV with the ATLAS experiment,” *Phys. Rev. D* **92** (2015) no. 5, 052002, [arXiv:1505.01609 \[hep-ex\]](#).
- [52] **CMS** Collaboration, A. M. Sirunyan *et al.*, “Search for an exotic decay of the Higgs boson to a pair of light pseudoscalars in the final state of two muons and two  $\tau$  leptons in proton-proton collisions at  $\sqrt{s} = 13$  TeV,” *JHEP* **11** (2018) 018, [arXiv:1805.04865 \[hep-ex\]](#).
- [53] **ATLAS** Collaboration, M. Aaboud *et al.*, “Search for Higgs boson decays to beyond-the-Standard-Model light bosons in four-lepton events with the ATLAS detector at  $\sqrt{s} = 13$  TeV,” *JHEP* **06** (2018) 166, [arXiv:1802.03388 \[hep-ex\]](#).
- [54] **CMS** Collaboration, A. M. Sirunyan *et al.*, “A search for pair production of new light bosons decaying into muons in proton-proton collisions at 13 TeV,” *Phys. Lett. B* **796** (2019) 131–154, [arXiv:1812.00380 \[hep-ex\]](#).
- [55] **CMS** Collaboration, V. Khachatryan *et al.*, “Search for light bosons in decays of the 125 GeV Higgs boson in proton-proton collisions at  $\sqrt{s} = 8$  TeV,” *JHEP* **10** (2017) 076, [arXiv:1701.02032 \[hep-ex\]](#).
- [56] **ATLAS Collaboration** Collaboration, “Exotic Higgs Decay Summary Plots,” Tech. Rep. ATL-PHYS-PUB-2018-045, CERN, Geneva, Dec, 2018. <http://cds.cern.ch/record/2650740>.
- [57] **ATLAS** Collaboration, M. Aaboud *et al.*, “Search for a heavy Higgs boson decaying into a Z boson and another heavy Higgs boson in the  $\ell\bar{\ell}bb$  final state in pp collisions at  $\sqrt{s} = 13$  TeV with the ATLAS detector,” *Phys. Lett. B* **783** (2018) 392–414, [arXiv:1804.01126 \[hep-ex\]](#).
- [58] **CMS** Collaboration, A. M. Sirunyan *et al.*, “Search for new neutral Higgs bosons through the  $H \rightarrow ZA \rightarrow \ell^+ \ell^- b\bar{b}$  process in pp collisions at  $\sqrt{s} = 13$  TeV,” [arXiv:1911.03781 \[hep-ex\]](#).
- [59] **CMS** Collaboration, V. Khachatryan *et al.*, “Search for neutral resonances decaying into a Z boson and a pair of b jets or  $\tau$  leptons,” *Phys. Lett. B* **759** (2016) 369–394, [arXiv:1603.02991 \[hep-ex\]](#).
- [60] **ALEPH, DELPHI, L3, OPAL, LEP Working Group for Higgs Boson Searches** Collaboration, S. Schael *et al.*, “Search for neutral MSSM Higgs bosons at LEP,” *Eur. Phys. J. C* **47** (2006) 547–587, [arXiv:hep-ex/0602042 \[hep-ex\]](#).
- [61] **ATLAS** Collaboration, M. Aaboud *et al.*, “Measurement of the  $t\bar{t}Z$  and  $t\bar{t}W$  cross sections in proton-proton collisions at  $\sqrt{s} = 13$  TeV with the ATLAS detector,” *Phys. Rev. D* **99** (2019) no. 7, 072009, [arXiv:1901.03584 \[hep-ex\]](#).
- [62] **CMS** Collaboration, A. M. Sirunyan *et al.*, “Search for production of four top quarks in final states with same-sign or multiple leptons in proton-proton collisions at  $\sqrt{s} = 13$  TeV,” [arXiv:1908.06463 \[hep-ex\]](#).
- [63] **ATLAS** Collaboration, M. Aaboud *et al.*, “Search for four-top-quark production in the single-lepton and opposite-sign dilepton final states in pp collisions at  $\sqrt{s} = 13$  TeV with the ATLAS detector,” *Phys. Rev. D* **99** (2019) no. 5, 052009, [arXiv:1811.02305 \[hep-ex\]](#).

- [64] **ATLAS** Collaboration, M. Aaboud *et al.*, “Search for new phenomena in events with same-charge leptons and  $b$ -jets in  $pp$  collisions at  $\sqrt{s} = 13$  TeV with the ATLAS detector,” *JHEP* **12** (2018) 039, [arXiv:1807.11883 \[hep-ex\]](#).
- [65] **ALEPH, DELPHI, L3, OPAL, SLD, LEP Electroweak Working Group, SLD Electroweak Group, SLD Heavy Flavour Group** Collaboration, S. Schael *et al.*, “Precision electroweak measurements on the  $Z$  resonance,” *Phys. Rept.* **427** (2006) 257–454, [arXiv:hep-ex/0509008 \[hep-ex\]](#).
- [66] J. Haller, A. Hoecker, R. Kogler, K. Mönig, T. Peiffer, and J. Stelzer, “Update of the global electroweak fit and constraints on two-Higgs-doublet models,” *Eur. Phys. J.* **C78** (2018) no. 8, 675, [arXiv:1803.01853 \[hep-ph\]](#).
- [67] **ATLAS** Collaboration, G. Aad *et al.*, “Search for a light charged Higgs boson in the decay channel  $H^+ \rightarrow c\bar{s}$  in  $t\bar{t}$  events using  $pp$  collisions at  $\sqrt{s} = 7$  TeV with the ATLAS detector,” *Eur. Phys. J.* **C73** (2013) no. 6, 2465, [arXiv:1302.3694 \[hep-ex\]](#).
- [68] **CMS** Collaboration, C. Collaboration, “Search for a light charged Higgs boson in the  $H^\pm \rightarrow cs$  channel at 13 TeV,”.
- [69] **ATLAS** Collaboration, M. Aaboud *et al.*, “Search for charged Higgs bosons decaying via  $H^\pm \rightarrow \tau^\pm \nu_\tau$  in the  $\tau$ +jets and  $\tau$ +lepton final states with  $36 \text{ fb}^{-1}$  of  $pp$  collision data recorded at  $\sqrt{s} = 13$  TeV with the ATLAS experiment,” *JHEP* **09** (2018) 139, [arXiv:1807.07915 \[hep-ex\]](#).
- [70] **CMS** Collaboration, A. M. Sirunyan *et al.*, “Search for charged Higgs bosons in the  $H^\pm \rightarrow \tau^\pm \nu_\tau$  decay channel in proton-proton collisions at  $\sqrt{s} = 13$  TeV,” *JHEP* **07** (2019) 142, [arXiv:1903.04560 \[hep-ex\]](#).
- [71] **ATLAS** Collaboration, M. Aaboud *et al.*, “Search for charged Higgs bosons decaying into top and bottom quarks at  $\sqrt{s} = 13$  TeV with the ATLAS detector,” *JHEP* **11** (2018) 085, [arXiv:1808.03599 \[hep-ex\]](#).
- [72] **CMS** Collaboration, A. M. Sirunyan *et al.*, “Search for a charged Higgs boson decaying into top and bottom quarks in events with electrons or muons in proton-proton collisions at  $\sqrt{s} = 13$  TeV,” *JHEP* **01** (2020) 096, [arXiv:1908.09206 \[hep-ex\]](#).
- [73] **HFLAV** Collaboration, Y. Amhis *et al.*, “Averages of  $b$ -hadron,  $c$ -hadron, and  $\tau$ -lepton properties as of summer 2016,” *Eur. Phys. J.* **C77** (2017) no. 12, 895, [arXiv:1612.07233 \[hep-ex\]](#).
- [74] S. Liebler, S. Patel, and G. Weiglein, “Phenomenology of on-shell Higgs production in the MSSM with complex parameters,” *Eur. Phys. J.* **C77** (2017) no. 5, 305, [arXiv:1611.09308 \[hep-ph\]](#).
- [75] D. Eriksson, J. Rathsman, and O. Stal, “2HDMC: Two-Higgs-Doublet Model Calculator Physics and Manual,” *Comput. Phys. Commun.* **181** (2010) 189–205, [arXiv:0902.0851 \[hep-ph\]](#).
- [76] **ATLAS** Collaboration, M. Aaboud *et al.*, “Search for heavy particles decaying into a top-quark pair in the fully hadronic final state in  $pp$  collisions at  $\sqrt{s} = 13$  TeV with the ATLAS detector,” *Phys. Rev.* **D99** (2019) no. 9, 092004, [arXiv:1902.10077 \[hep-ex\]](#).
- [77] B. Coleppa, F. Kling, and S. Su, “Exotic Higgs Decay via  $AZ/HZ$  Channel: a Snowmass Whitepaper,” [arXiv:1308.6201 \[hep-ph\]](#).
- [78] B. Coleppa, F. Kling, and S. Su, “Charged Higgs search via  $AW^\pm/HW^\pm$  channel,” *JHEP* **12** (2014) 148, [arXiv:1408.4119 \[hep-ph\]](#).
- [79] B. Coleppa, F. Kling, and S. Su, “Exotic Decays Of A Heavy Neutral Higgs Through  $HZ/AZ$  Channel,” *JHEP* **09** (2014) 161, [arXiv:1404.1922 \[hep-ph\]](#).
- [80] J. Hajer, A. Ismail, F. Kling, Y.-Y. Li, T. Liu, and S. Su, “Searches for non-SM heavy Higgses at a 100 TeV  $pp$  collider,” *Int. J. Mod. Phys.* **A30** (2015) no. 23, 1544005.
- [81] F. Kling, A. Pyarelal, and S. Su, “Light Charged Higgs Bosons to  $AW/HW$  via Top Decay,” *JHEP* **11** (2015) 051, [arXiv:1504.06624 \[hep-ph\]](#).
- [82] F. Kling, H. Li, A. Pyarelal, H. Song, and S. Su, “Exotic Higgs Decays in Type-II 2HDMs at the LHC and Future 100 TeV Hadron Colliders,” *JHEP* **06** (2019) 031, [arXiv:1812.01633 \[hep-ph\]](#).
- [83] P. M. Ferreira, J. F. Gunion, H. E. Haber, and R. Santos, “Probing wrong-sign Yukawa couplings at the LHC and a future linear collider,” *Phys. Rev.* **D89** (2014) no. 11, 115003, [arXiv:1403.4736 \[hep-ph\]](#).
- [84] W. Su, “Probing loop effects in wrong-sign Yukawa region of 2HDM,” [arXiv:1910.06269 \[hep-ph\]](#).
- [85] X.-F. Han, “Revisiting wrong sign Yukawa coupling of type II two-Higgs-doublet model in light of the recent LHC data,” [arXiv:2003.06170 \[hep-ph\]](#).
- [86] W.-S. Hou and T. Modak, “Prospects for  $tZH$  and  $tZh$  production at the LHC,” *Phys. Rev.* **D101** (2020) no. 3, 035007, [arXiv:1911.06010 \[hep-ph\]](#).
- [87] S. Baum, K. Freese, N. R. Shah, and B. Shakya, “NMSSM Higgs boson search strategies at the LHC and the mono-Higgs signature in particular,” *Phys. Rev.* **D** **95** (2017) no. 11, 115036, [arXiv:1703.07800 \[hep-ph\]](#).
- [88] S. Baum and N. R. Shah, “Two Higgs Doublets and a Complex Singlet: Disentangling the Decay Topologies and Associated Phenomenology,” *JHEP* **12** (2018) 044, [arXiv:1808.02667 \[hep-ph\]](#).
- [89] S. Baum, N. R. Shah, and K. Freese, “The NMSSM is within Reach of the LHC: Mass Correlations & Decay Signatures,” *JHEP* **04** (2019) 011, [arXiv:1901.02332 \[hep-ph\]](#).
- [90] S. Baum and N. R. Shah, “Benchmark Suggestions for Resonant Double Higgs Production at the LHC for Extended Higgs Sectors,” [arXiv:1904.10810 \[hep-ph\]](#).